

## **Measurement of the Longitudinal Wakefield in the SLAC Linac for Extremely Short Bunches \***

K. Bane, F.-J. Decker, P. Emma, L. Hendrickson, P. Krejcik,  
C.L. O'Connell, H. Schlarb,<sup>†</sup> J. Welch, M. Woodley  
*Stanford Linear Accelerator Center, Stanford University,  
Stanford, CA 94309 USA*

*Presented at the 2003 Particle Accelerator Conference (PAC'03),  
Portland, OR May 12-16, 2003*

---

\*Work supported by Department of Energy contract DE-AC03-76SF00515.

<sup>†</sup>Visitor from DESY.

# Measurement of the Longitudinal Wakefield in the SLAC Linac for Extremely Short Bunches\*

K. Bane, F.-J. Decker, P. Emma, L. Hendrickson, P. Krejcik, C.L. O'Connell, H. Schlarb,<sup>†</sup>  
J. Welch, M. Woodley: Stanford Linear Accelerator Center, Stanford, CA 94309, USA

## INTRODUCTION

The Linac Coherent Light Source (LCLS) [1] is an x-ray FEL project with a 1-nC electron bunch compressed to an rms length of 20 microns at 4.5 GeV, accelerated in 500 meters of SLAC linac to 15 GeV, and then injected into an undulator to generate SASE radiation. The longitudinal wakefield generated by the short bunch in the (S-band) linac is very strong, and is relied upon to cancel the energy chirp left in the beam after bunch compression.

Up to now, both the average [2] and the shape [3] of the longitudinal wake of the SLAC linac have been measured and confirmed using bunches ranging down to an rms 500-microns in length. The recent installation of a chicane in the SLAC linac for the Sub-Picosecond Photon Source (SPPS) [4, 5, 6], however, allows compression of a 3.4-nC bunch down to 50  $\mu\text{m}$  rms length. We present measurements of the average wakefield, for bunch lengths down to this, LCLS-type scale, and compare with theory.

## THEORY

For a periodic, disk-loaded structure the steady-state longitudinal wakefield can be obtained numerically. The result over the very short-range can be approximated by [7]

$$W(s) = \frac{Z_0 c}{\pi a^2} H(s) e^{-\sqrt{s/s_0}}, \quad (1)$$

where  $s$  is the longitudinal separation between drive and test particles ( $s > 0$  if the drive particle leads); with  $Z_0 = 377 \Omega$ ,  $c$  the speed of light,  $a$  the (average) structure iris radius; with  $H(s) = 1$  (0) if  $s > 0$  ( $< 0$ ). The parameter  $s_0 = 0.41g^{1.6}a^{1.8}/p^{2.4}$  with  $g$  the gap length and  $p$  the period length. For the SLAC linac structure,  $a = 1.16$  cm,  $g = 2.92$  cm, and  $p = 3.50$  cm;  $s_0 = 1.47$  mm and the model is valid for  $s \lesssim 5$  mm. Note that Eq. (1) gives the steady-state solution, valid after the distance  $L_{crit} \approx \frac{1}{2}a^2/\sigma_z$ , after which initial transients have died down. For  $\sigma_z = 50 \mu\text{m}$ ,  $L_{crit} = 1.4$  m, which is very small compared to the total structure length; thus, the transient contribution is small and can be ignored.

We will describe measurements that depend on the average wake. For a Gaussian bunch with rms length  $\sigma_z$ , the loss factor—the average wake-induced energy loss per unit charge per unit length of structure—is given by

$$\kappa(\sigma_z) = \frac{1}{2\sqrt{\pi}\sigma_z} \int_0^\infty W(s) e^{-(s/\sigma_z)^2/4} ds. \quad (2)$$

Substituting Eq. (1) into Eq. (2) we obtain a result that can be approximated (for  $\sigma_z \lesssim s_0$  to 2% accuracy) by

$$\kappa(\sigma_z) \approx \frac{Z_0 c}{2\pi a^2} e^{-0.88\sqrt{\sigma_z/s_0}}. \quad (3)$$

The average energy gain of a bunch after passing through a linac is given by a combination of the applied rf and the wakefield effect. The average gain of a Gaussian bunch is

$$\Delta E = \hat{E}_{acc} \cos \phi e^{-k_{rf}^2 \sigma_z^2 / 2} - eNL\kappa(\sigma_z), \quad (4)$$

with  $\hat{E}_{acc}$  the crest energy change,  $\phi$  the average bunch phase (with respect to crest),  $k_{rf}$  the rf wave number,  $eN$  the bunch charge, and  $L$  the total structure length. Note that increasing the bunch length will decrease the first and increase the second term contributions, and the converse is also true. Note also that when  $\sqrt{\sigma_z/s_0} \ll 1$  we lose sensitivity in  $\Delta E$  to bunch length.

To estimate the range of energy change that we can expect to measure, consider first that, for a point charge, the total wake effect is  $(eNLZ_0c)/(2\pi a^2)$ , which in our experiment is  $\sim 850$  MeV (3% of the final beam energy). For a bunch length range between 50 and 600  $\mu\text{m}$  this quantity is reduced by the difference of  $e^{-0.88\sqrt{\sigma_z/s_0}}$  at the two bunch lengths, yielding an energy change of  $\sim 240$  MeV (a 0.8% effect). Eqs. (3-4) can be used to estimate the wakefield effect for the measurements to be discussed. In reality the beams are not exactly Gaussians, however, and in the simulations used in comparisons to follow, no such assumption is made.

## MACHINE LAYOUT

A new four-dipole bunch compressor chicane was installed in sector-10 of the SLAC linac in October of 2002 [4, 5]. The chicane is located at the 1-km point in the 3-km linac, at 9 GeV. The electron bunch is extracted from a damping ring which is followed by an existing ring-to-linac (RTL) bunch compressor beamline at 1.2 GeV. The RTL includes a 2.1-m long S-band rf accelerating structure operated at the zero-crossing phase, followed by a series of bends which generate an  $R_{56}$  of 590 mm. The RTL structure is operated at a nominal voltage ( $V_{RTL}$ ) of 42 MV, which can vary with machine configuration.

A 3.4-nC bunch is compressed from 6-mm rms in the ring to 1.2-mm in the RTL, accelerated to the chicane at 9 GeV through 810-m of linac at an rf phase of  $-19^\circ$  (crest at 0), and then further compressed in the new chicane to as short as 50- $\mu\text{m}$  rms (up to 9-kA peak current). The time-correlated energy spread at chicane entrance is 1.6% rms,

\* Work supported by U.S. Department of Energy, contract DE-AC03-76SF00515.

<sup>†</sup> Visitor from DESY.

with bunch head at lower energy than its tail. The bunch is then accelerated to 28.5 GeV in 1870 meters of S-band rf accelerating structures, where in order to save power, only  $\sim 90$  of the 160 available klystrons beyond the chicane are presently switched on. Figure 1 shows the machine layout.

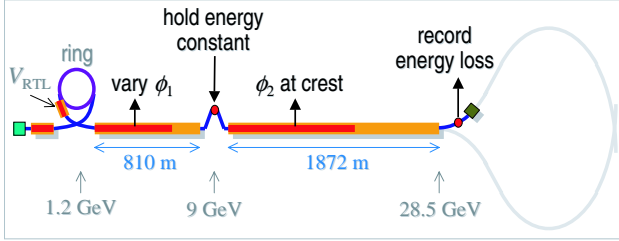


Figure 1: Layout of ring, RTL, linac, and chicane. Linac sections highlighted in red are rf-powered.

The longitudinal wakefield of the post-chicane linac generates an energy loss and spread which reaches a maximum for the shortest bunch length. This dependence can be used to find the minimum bunch length by maximizing the energy loss. This is done by varying the pre-chicane rf phase ( $\phi_1$ ), composed of the first 40 klystrons in sectors 2-6, several degrees around its nominal setting of  $-19^\circ$ , while the chicane energy is held constant. The varying phase changes the correlated energy spread in the chicane, which changes the final bunch length, passing through a minimum near  $-19^\circ$  with over- and under-compression on either side.

The energy in the chicane is held constant by a pair of “feedback” klystrons in sector-9, each operated symmetrically around opposing zero-crossing phases (at  $\pi/2 \pm \Delta\phi_f$  and  $-\pi/2 \mp \Delta\phi_f$ ). This allows energy control without changing the correlated energy spread. A beam position monitor (BPM) at the center of the chicane is used to drive this micro-processor based chicane energy-feedback system. With a peak  $x$ -dispersion of 450 mm in the chicane and a  $50\text{-}\mu\text{m}$  BPM resolution, the single-shot energy resolution is 0.01%, or 1 MeV. The actual pulse-to-pulse energy stability in the chicane is typically 0.05%, or 5 MeV rms.

A second BPM, located after a bend at the end of the linac, is used to record energy change as a function of  $\phi_1$ . The 5-MeV chicane energy stability, and its  $R_{56}$  of  $-76$  mm, contributes to post-chicane rf phase ( $\phi_2$ ) errors of  $< 0.2^\circ$  around crest phase. This tiny error is  $< 0.2$  MeV at the end of the linac. Therefore, any significant energy change at the end of the linac, which is correlated with  $\phi_1$ , minus the chicane energy error, is due to the bunch-length dependent wakefield in the post-chicane linac.

The shortest bunch length is produced at the  $\phi_1$  phase where the energy loss is maximized. This simple procedure has become a standard optimization and diagnostic tool to quickly (2-3 minutes) minimize the bunch length after the chicane, at any bunch charge and with any  $V_{RTL}$  setting.

## SIMULATIONS

Particle tracking from ring extraction to end-of-linac has been done in 2D (longitudinal only), and also confirmed in 6D. More tracking details are shown in reference [5]. Machine and beam parameters are given in Table 1. The tracking starts at ring extraction with a gaussian energy profile and a slightly asymmetric-gaussian temporal profile, due to resistive ring vacuum chamber impedance [6, 9].

Table 1: Machine and electron bunch parameters.

bunch population	$N$	1.8-2.1	$10^{10}$
$e^-$ energy in ring	$E_0$	1.19	GeV
ring rms energy spread	$\sigma_E/E_0$	0.08	%
ring rms bunch length	$\sigma_{z_0}$	6.0	mm
pre-chicane rf phase	$\phi_1$	$-19$	deg
post-chicane rf phase	$\phi_2$	0	deg

The tracking includes 1st, 2nd, and 3rd-order momentum compaction ( $R_{56}$ ,  $T_{566}$ , and  $U_{5666}$ ) in the RTL and chicane. It also includes sinusoidal rf, and longitudinal geometric wakefields of all rf structures: before and after the chicane, and in the RTL. Figure 2 shows simulated longitudinal phase space, energy, and temporal distributions after the chicane and after the full linac, for the minimum bunch length. A gaussian-fit (in red) is used to determine the core bunch length at  $\sigma_z \approx 40 \mu\text{m}$  rms. The energy spread is uncorrelated immediately after the chicane, but the wakefield of the post-chicane linac induces a large correlated spread and a mean loss of  $\sim 1\%$  (bunch head at left here).

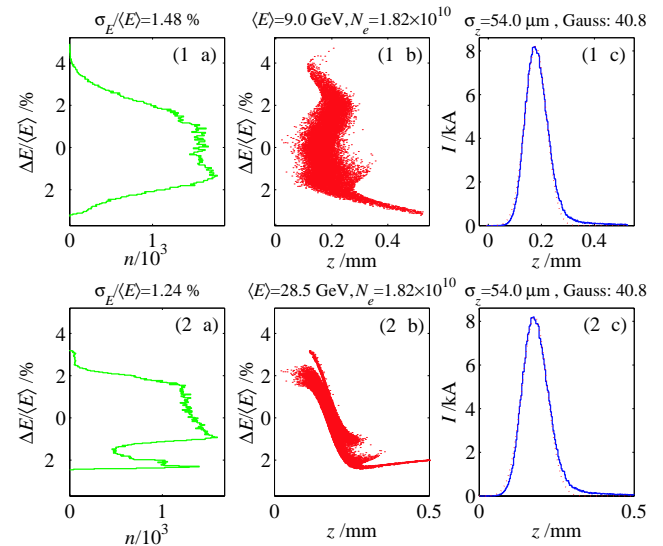


Figure 2: Beam at chicane exit (top) and end of linac (bottom), showing longitudinal phase space (1-b & 2-b), energy (1-a & 2-a), and temporal (1-c & 2-c) distributions (gaussian-fit in red:  $\sigma_z \approx 40 \mu\text{m}$  rms).

Incoherent synchrotron radiation in the 9-GeV chicane bends is also included, but is a small effect producing an rms energy spread of 0.006% and a loss of 0.02% at 9 GeV.

The effects of coherent synchrotron radiation (CSR) in the chicane have also been calculated and, although there is a small effect on the  $x$ -emittance [10], the maximum rms energy spread and mean loss due to CSR is very small at 0.02 and 0.03%, respectively (at 9 GeV with 3.4 nC).

Finally, a small  $V_{RTL}$ -dependent beam loss in the narrow-aperture RTL beamline is also included in the simulations. Transmission measurements at various  $V_{RTL}$  settings (various  $x$  beam sizes in the RTL) show the energy-aperture at  $\pm 2\%$ . At 3 nC and  $V_{RTL} = 42$  MV, this results in a 9% particle loss (7% at 40 MV and 12% at 45 MV).

The simulations are run multiple times with  $\phi_1$  varied  $\pm 7^\circ$  in  $0.5^\circ$  steps, around the nominal phase of  $-19^\circ$ , with chicane energy held constant. The energy change at the end of the linac vs.  $\phi_1$  is compared with measurements.

## MEASUREMENTS

The energy loss of the compressed bunch is measured by reading the computations of a second micro-processor based energy-feedback system which nominally holds the electron energy constant at the end of the linac. This system uses three BPMs, one placed after a bend magnet with ( $x$ )-dispersion  $\eta_x \approx -86$  mm, and the other two, prior to the bend, at  $\eta_x = 0$ , to accommodate trajectory variations initiated upstream of the bend. BPM calibration was verified accurate to 5%. The feedback loop is switched to “compute-only” mode during the wake-loss scans, which calculates energy, but applies no correction.

As described above, the rf phase,  $\phi_1$ , is varied while the chicane energy is held constant, and the end-of-linac energy is monitored. The final energy is typically stable to 8 MeV rms (0.03%) and five beam pulses (10 Hz) are averaged per  $\phi_1$  setting for a measurement error of 4 MeV.

The final bunch length was confirmed using a transverse deflecting rf structure to ‘streak’ the beam on an off-axis screen [11]. The absolute bunch length is measured from the streaked vertical beam size and independently demonstrates a minimum rms bunch length of  $60 \pm 10$   $\mu\text{m}$ .

The measured and simulated energy loss vs.  $\phi_1$  settings are shown in Figures 3. Each scan is at a different RTL voltage (40 to 45 MV). The error bars show the estimated rms energy stability at each point. For this data taken at 3.0 nC, an RTL voltage other than 42 MV results in a longer minimum bunch length and a different correlated energy spread in the chicane. Therefore, the depth of the energy loss and the phase at the minimum will change for each RTL voltage setting. The (c) plot (42 MV) also shows the rms simulated bunch length (dotted), with scale at far right.

No fitting parameters are used, except the arbitrary offset on the vertical (energy) scale. The measurements and simulations are simply overlaid. The nominal 42 MV case (c) agrees quite well, but the 40 and 41 MV settings, (a) and (b), show a flat-bottomed area which is not understood. There also appears to be a slight RTL-saturation effect at  $V_{RTL} > 42$  MV. The dashed curves in (d), (e) and (f) show the simulation at the actual  $V_{RTL}$  settings, but the data suggests that the RTL klystron was beginning to saturate here.

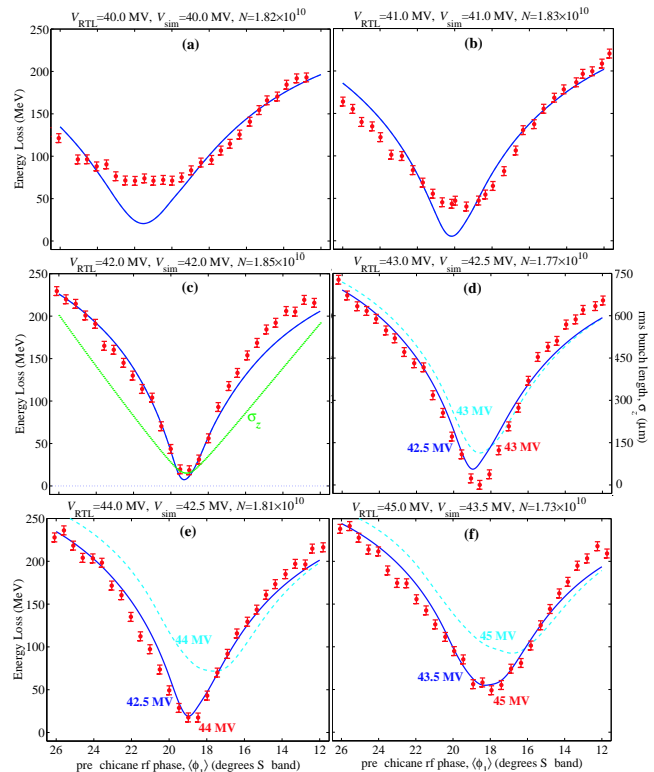


Figure 3: Wake-loss scans (the vertical scale has an arbitrary offset) with varying  $V_{RTL}$  from 40 to 45 MV, (a) to (f), respectively. The 42-MV case (c) also plots the simulated rms bunch length: scale at far right.

At the setting of 43 MV in (d), the data fits slightly better to 42.5 MV (solid). Likewise, at 44 and 45 MV settings in (e) and (f), the data fits much better to 42.5 and 43.5 MV, respectively. Note especially the measurements at 42 (c), 43 (d), and 44 MV (e) are almost identical, yet the simulations (dashed) at 43 and 44 MV suggest a clear change should have occurred. Unfortunately, this klystron saturation possibility was not confirmed by any independent technique. Further measurements, including wakefield-induced energy spread, will be made in the near future.

## REFERENCES

- [1] *LCLS CDR*, SLAC Report No. SLAC-R-593, 2002.
- [2] K. Bane, *et al.*, EPAC’90, Nice, France, June 1990, p. 1762.
- [3] K.L.F. Bane, *et al.*, PAC’97, Vancouver, May 1997, p. 1876.
- [4] P. Krejcik, *et al.*, *Commissioning of the SPPS Linac Bunch Compressor*, PAC’03, Portland, OR, May 2003.
- [5] L. Bentson *et al.*, EPAC’02, Paris, France, June 2002, p. 683.
- [6] P. Emma, *et al.*, PAC’01, Chicago, USA, June 2001, p. 4038.
- [7] K.L.F. Bane, *et al.*, ICAP’98, Monterey, Sept. 1998, p. 137.
- [8] K.L.F. Bane, *et al.*, PAC’97, Vancouver, May 1997, p. 515.
- [9] K. Bane, *et al.*, PAC’95, Dallas, TX, June 1995, p. 3109.
- [10] P. Emma, *et al.*, *Measurements of Transverse Emittance Growth due to ...*, PAC’03, Portland, OR, May 2003.
- [11] R. Akre, *et al.*, EPAC’02, Paris, France, June 2002, p. 1882.